NEW ALGORITHMS FOR FAST AND ACCURATE AM-FM DEMODULATION OF DIGITAL IMAGES

Paul Rodríguez V. and Marios S. Pattichis

The University of New Mexico
Department of Electrical and Computer Engineering
Albuquerque, N.M. 87111, U.S.A.

ABSTRACT

Multidimensional Amplitude-Modulation Frequency - Modulation (AM-FM) models allow us to describe continuous-scale modulations in digital images. AM-FM models have led to a wide range of applications ranging from image and video compression, video image segmentation, to image retrieval in digital libraries. We present new, two-dimensional algorithms that provide significant improvements in both accuracy and speed over previously reported non-parametric approaches. Results are shown for both real and synthetic images.

1. INTRODUCTION

Multidimensional AM-FM models provide methods that allow for continuous-scale analysis in digital images. Recent applications of the AM-FM model range from image interpolation [1], fingerprint classification [2], image segmentation [3], and video segmentation [4]. Thus, there is strong interest in the development of fast and accurate AM-FM demodulation methods. We expect that all prior applications of AM-FM demodulation can benefit from the use of the proposed algorithms.

For general AM-FM expansions of images, we have:

$$I(x,\, y) = \sum_{n=1}^{n=M} a_n(x,\, y) \cos\, \varphi_n(x,\, y). \tag{1}$$

In (1), an image $I(.)$ is a function of spatial coordinates $(x,\, y)$. A collection of M AM-FM component images $a_n(x,\, y)$ $\cos \varphi_n(x,\, y)$, $n = 1, 2, \ldots, M$ is used to model essential image modulation structure. The amplitude functions $a_n(x,\, y)$ are always assumed to be non-negative. We expect that the Frequency-Modulated components $\cos \varphi_n(x,\, y)$ will capture fast-changing spatial variability in image intensity. The instantaneous frequency is a vector field defined in terms of the gradient of each phase function:

$$\nabla \varphi_n(x,\, y) = \left(\frac{\partial \varphi_n}{\partial x}(x,\, y),\, \frac{\partial \varphi_n}{\partial y}(x,\, y) \right). \tag{2}$$

The instantaneous frequency vector $\nabla \varphi_n(x,\, y)$ can vary continuously over the spatial domain of the image. We will only consider the dominant component approximation [5], where a single AM-FM component is used to approximate any given image. We thus consider the AM-FM demodulation problem which requires that we estimate the instantaneous amplitude (IA) $a(x,\, y)$, the phase $\varphi(x,\, y)$, and the instantaneous frequency vector (IF) $\nabla \varphi(x,\, y)$ from any given image.

We develop new algorithms based on multidimensional extensions of the analytic signal. Our approach is motivated by the fact that the analytic signal approach can be shown to be the unique approach that satisfies certain intuitive criteria, including stability criteria, as shown in [6] and extended in [5].

We summarize existing image demodulation methods in section 2. New AM-FM demodulation methods are presented in section 3, and comparative results are shown in section 4. Concluding remarks are given in section 5.

2. IMAGE DEMODULATION METHODS

For any given image $f(.)$, we compute a two-dimensional analytic signal, as given in [5]:

$$f_{AS}(x,\, y) = f(x,\, y) + j\mathcal{H}_{2d}[f(x,\, y)], \tag{3}$$

where $\mathcal{H}_{2d}$ denotes the one-dimensional Hilbert transform operator applied along the rows (or columns). We estimate the amplitude, the phase, and the instantaneous frequency using

$$a(x,\, y) = |f_{AS}(x,\, y)|, \tag{4}$$

$$\varphi(x,\, y) = \arctan\left(\frac{\mathrm{imag}(f_{AS}(x,\, y))}{\mathrm{real}(f_{AS}(x,\, y))} \right), \quad \text{and} \tag{5}$$

$$\omega(x,\, y) = \mathrm{real}\left[-j \frac{\nabla f_{AS}(x,\, y)}{f_{AS}(x,\, y)} \right]. \tag{6}$$

The algorithm can be summarized into two steps. First, we compute the analytic signal using (3). Second, we compute

0-7803-9134-9/05/$20.00 ©2005 IEEE

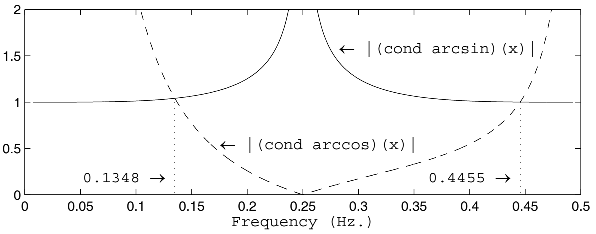

Fig. 1. Absolute value of the condition number for the arc-cosine (dash line) and arc-sine (solid line) are shown. The x-axis refers to 0.5 multiplied by the sampling frequency. Both condition numbers are equal at 0.1348 and 0.4455.

all the estimates using (4), (5), (6). A discrete-space extension of the algorithm can be developed using the quasi eigenfunction approximation [7]. This leads to the following formulas for estimating the instantaneous frequency vectors:

$$\frac{\partial \varphi}{\partial x}(k_1,\, k_2) \approx \arcsin\left[\frac{f_{AS}(k_1+1,\, k_2) - f_{AS}(k_1-1,\, k_2)}{2j f_{AS}(k_1,\, k_2)}\right], \tag{7}$$

$$\frac{\partial \varphi}{\partial y}(k_1,\, k_2) \approx \arcsin\left[\frac{f_{AS}(k_1,\, k_2+1) - f_{AS}(k_1,\, k_2-1)}{2j f_{AS}(k_1,\, k_2)}\right], \tag{8}$$

$$\frac{\partial \varphi}{\partial x}(k_1,\, k_2) \approx \arccos\left[\frac{f_{AS}(k_1+1,\, k_2) + f_{AS}(k_1-1,\, k_2)}{2 f_{AS}(k_1,\, k_2)}\right], \tag{9}$$

$$\frac{\partial \varphi}{\partial y}(k_1,\, k_2) \approx \arccos\left[\frac{f_{AS}(k_1,\, k_2+1) + f_{AS}(k_1,\, k_2-1)}{2 f_{AS}(k_1,\, k_2)}\right]. \tag{10}$$

To recognize the instabilities associated with (7)-(10), we compute the condition numbers for $\arcsin(.)$, $\ldots$, $\arccos(.)$ for different instantaneous frequencies (see section 3.1).

3. FAST AND ACCURATE DEMODULATION OF DIGITAL IMAGES

In subsection 3.1, we begin with a brief summary of how to extend the demodulation method of section 2 to become robust. In section 3.2, we present a novel, two-dimensional AM-FM demodulation method based on the quasi-local method of [8]. A general discussion on fast implementations is given in section 3.3.

3.1. Robust Demodulation Using the Quasi-Eigenfunction Approximation

It can be shown that the quasi-eigenfunction approximation described in (7)-(10) is numerically unstable. To show this, we compute the condition numbers of each one of the inverse trigonometric functions, and note that they can grow unbounded at different frequencies (also see [9] for the definition of the condition number). However, it turns out that the functions are unbounded over different, discrete fourier frequencies (see Figure 1). Thus, a robust demodulation algorithm can be designed that chooses between (7) and (9) and also between (8) and (10) for estimating the components of the instantaneous-frequency. We will later show that dramatic improvements are possible using this approach.

3.2. Continuous-Space, Multidimensional Demodulation for the Quasi-Local Method

To develop the new algorithm, we first assume that the input image is a single AM-FM harmonic $f(x,\, y) = a(x,\, y)$ $\cos\varphi(x,\, y)$. For estimating the IA, we first note that

$$2f^2(x,y) = a^2(x,y) + a^2(x,y)\cos(2\varphi(x,y)). \tag{11}$$

Thus, if we use a lowpass filter $h(.)$ to reject the second term in (11), we get the IA estimate

$$\hat{a}(x,y) = \sqrt{2f^2(x,y) * h(x,y)}. \tag{12}$$

We define

$$g_x(\epsilon_1,\epsilon_2) = f(x+\epsilon_1,y)f(x-\epsilon_2,y). \tag{13}$$

which reduces to

$$g_x(\epsilon,\epsilon) = \frac{a_x(\epsilon,\epsilon)}{2}\cos\left(\varphi(x+\epsilon,y) - \varphi(x-\epsilon,y)\right) + \frac{a_x(\epsilon,\epsilon)}{2}\cos\left(\varphi(x+\epsilon,y) + \varphi(x-\epsilon,y)\right) \tag{14}$$

where $a_x(\epsilon_1,\epsilon_2) = a(x+\epsilon_1,y)a(x-\epsilon_2,y)$. The basic assumption for IF estimation is that we can design a lowpass filter to reject the second term in (14). Similarly, we use the same lowpass filter to filter out the second terms from the expansions of $g_x(\epsilon,\, 0)$ and $g_x(0,\epsilon)$. We note that the lowpass filter must be chosen so that it contains the desired AM-FM component, for a single, dominant component. In the presence of multicomponent signals, we must rely on prior, bandpass filtering, where the basic assumption is that there is only one AM-FM component coming out of each band.

Define R_x by

$$R_x(\epsilon) = \frac{2h(x,\, y) * \{g_x(\epsilon,\epsilon)\}}{h(x,\, y) * \{g_x(\epsilon,0) + g_x(0,\epsilon)\}} \tag{15}$$

Using R_x, we can get an IF estimate along the x-component using

$$\left|\frac{\partial\varphi(x,\, y)}{\partial x}\right| = \lim_{\epsilon\to 0^+}\left\{\frac{1}{\epsilon}\arccos\left(\frac{R_x(\epsilon) + \sqrt{R_x^2(\epsilon)+8}}{4}\right)\right\}.$$

The discrete-space algorithm follows directly by considering a discrete lattice for x, y, so that $(x, y) = (n\Delta x, m\Delta y)$, for $n, m \in \mathbb{Z}$ and for ϵ to be some positive integral multiple of Δx. For the y-dimension, a similar approach can be taken. Furthermore, it is straight-forward how to extend the algorithm for any finite number of dimensions.

To estimate the signs of the IF vector components, we use a hybrid approach that uses (6) to determine the sign. Furthermore, in our hybrid approach, we use (5) for estimating the phase.

3.3. Fast Implementations

Fast implementation of the AM-FM demodulation algorithm is based on separable, one-dimensional implementations of the lowpass and bandpass filters involved. Furthermore, fast convolutions can be computed using the SIMD-FFT, an adaptation of the fastest FFT algorithm to run on the Single Instruction Multiple Data (SIMD) units of general-purpose processors [10], [11]. We note that separable implementations provide linear memory access and can yield significant speed improvements over non-separable implementations. Also, SIMD implementations can yield speedups of the order of the number of packed data elements that are processed in parallel. Currently, this yields a four-fold increase in speed [10], [11].

4. RESULTS

In this section, we present three sets of results. We present comparative results from a one-dimensional chirp signal, demodulation from a two-dimensional chirp image, and a real-life example.

In table 1, we present comparative results for a noisy chirp signal. We note that for all methods two bandpass filters were used, and the resulting estimates were taken from the filter that gave the largest response at each sample (dominant component analysis) [5]. Let $f(k) = \sin(2\pi \cdot (0.01 + 0.5 \cdot \xi(k)) \cdot k) + 0.05 \cdot \eta(k)$ be the input signal, where $\xi(k) = \frac{0.49}{N}k$ and $k \in [0, N-1]$, with $\eta \sim \mathcal{N}(0, 1)$, and $N = 512$. The analytic signal was computed via the Discrete Fourier Transform (first row) and Hilbert transformer (second row) using 31 coefficients. In the third row of the table, we present the results when using the Hilbert Transformer with the robust extension of section 3.1. The results for the IF and IA estimation of the proposed hybrid method of section 3.2 are shown in the fourth and last rows, respectively.

We note the significant improvements in both IF and IA estimation. The improvements in the IA estimation are due to the accurate estimation of the IF, because both IA amplitudes are obtained by dividing the output of the bandpass filters by their magnitude response at the IF.

	MSE($\hat{\omega} - \omega$)	$\|\hat{\omega} - \omega\|_2$	VAR($\frac{\hat{\omega}-\omega}{\omega}$)
IF using FFT	0.002026	1.017	5.726
IF using Hil.	0.001294	0.812	4.804
Robust IF	0.000968	0.703	0.366
Hybrid IF	0.000006	0.055	0.010
	MSE(â - a)	$\|$ â - a $\|_2$	VAR($\frac{\hat{a}-a}{a}$)
Basic IA	0.019	3.107	0.019
Hybrid IA	0.005	1.585	0.005

Table 1. Performance measurements for instantaneous amplitude (IA) and instantaneous frequency (IF) estimation.

All 2D examples are computed using spatial-convolutions and four bands. Using separable implementations with 1D filters with 30 taps, for 512×512 images, the proposed algorithm requires approximately 0.2 seconds per band, on a 3 GHz Pentium4 (L2 cache 512k) using Linux (kernel 2.6.10). A two-dimensional chirp example is presented in Figure 2. The reconstruction error is relatively low, with the exception of very low frequencies (see figure 2(c)). A real-life image example is presented in figure 3. From the reconstruction of figure 3(d), we see that the image is approximated rather well by the single AM-FM harmonic. As shown in the needle plot, high magnitude IF vectors are measured over the tree-rings and the edges of the tree, while low magnitude IF components are measured in the region outside the rings.

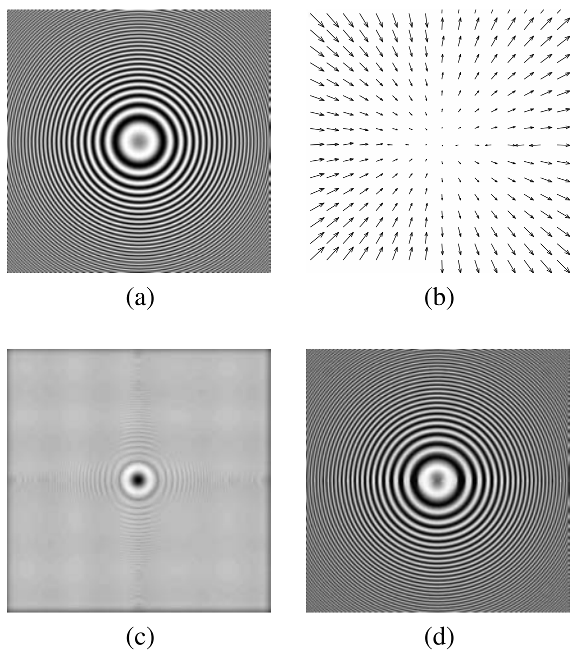

Fig. 2. Radial Chirp: (a) original image, (b) downsampled IF needle plot, (c) IA, and (d) reconstructed image.

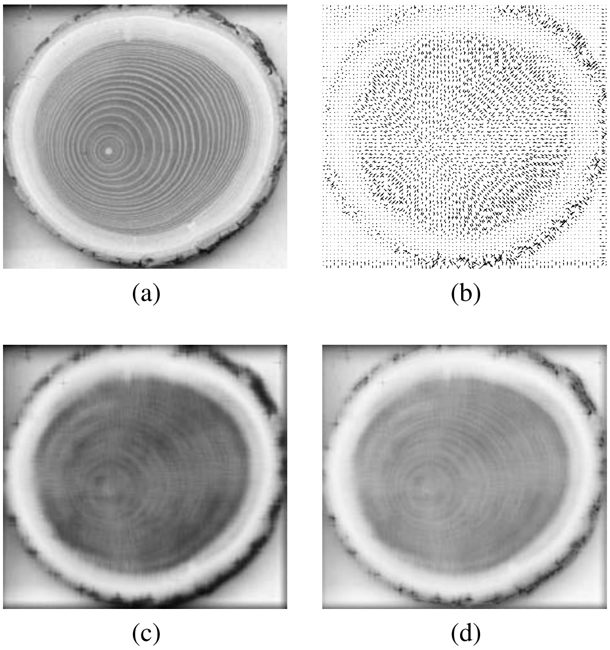

Fig. 3. Red oak: (a) original image , (b) IF needle plot , (c) IA and (d) reconstructed image (photo © H.D. Grissino-Mayer, http://web.utk.edu/ grissino/gallery.htm).

5. CONCLUSION

We presented novel methods for non-parametric AM-FM demodulation of digital images. The algorithms were shown to be fast and more robust than existing algorithms. We believe that a wide range of applications can benefit from faster and robust methods of image demodulation. Clearly, all prior applications that were based on AM-FM demodulation can benefit from using the algorithms presented in this paper.

6. REFERENCES

[1] S. T. Acton, D. P. Mukherjee, J. P. Havlicek, and A. C. Bovik, "Oriented texture completion by am-fm reaction-diffusion," *IEEE Trans. Image Processing*, vol. 10, no. 6, pp. 885–896, june 2001.

[2] M. Pattichis, G. Panayi, A. Bovik, and H. Shun-Pin, "Fingerprint classification using and am-fm model," *IEEE Trans. Image Processing*, vol. 10, no. 6, pp. 951–954, june 2001.

[3] M. Pattichis, C. Pattichis, M. Avraam, A. Bovik, and K. Kyriakou, "Am-fm texture segmentation in electron microscopic muscle imaging," *IEEE Trans. Med. Imag.*, vol. 19, no. 12, pp. 1253–1258, december 2000.

[4] P. Rodriguez V., M. Pattichis, and M. Goens, "M-mode echocardiography image and video segmentation based on am-fm demodulation techniques," in *Proc. of the 25th Intern. Conf. of the IEEE Engineering in Medicine and Biology Society (EMBS 2003)*, vol. 2, september 2003, pp. 1176–1179.

[5] J. P. Havlicek, "AM-FM image models," Ph.D. dissertation, The University of Texas at Austin, 1996.

[6] D. Vakman, *Signals, Oscillations, and Waves: A Modern Approach*. Boston: Artech House, 1998.

[7] J. P. Havlicek, D. S. Harding, and A. C. Bovik, "Multidimensional quasi-eigenfunction approximations and multicomponent am-fm models," in *IEEE Trans. Image Processing*, vol. 9, no. 2, february 2000, pp. 227–242.

[8] G. Girolami and D. Vakman, "Instantaneous frequency estimation and measurement: a quasi-local method," *Measurement Science Technology*, vol. 13, pp. 909–917, june 2002.

[9] S. D. Conte and C. de Boor, *Elementary Numerical Analysis: An ALgorithmic Approach*. McGrawHill, 1980.

[10] P. Rodriguez V., "A radix-2 fft algorithm for modern single instruction multiple data (simd) architectures," in *Proc. IEEE Intern. Conf. on Acoustics, Speech, and Signal Processing,(ICASSP 2002)*, vol. 3, may 2002, pp. III–3220 – III–3223.

[11] P. Rodriguez V., M. Pattichis, and R. Jordan, "Computational simd framework: split-radix simd-fft algorithm, derivation, implementation and performance," in *14th Intern. Conf. on DSP*, vol. 2, july 2002, pp. 861–864.